Journal of Structural Chemistry, Vol. 39, No. 6, 1998

DYNAMIC EFFECT ON THE STRUCTURE OF X-RAY PHOTOELECTRON SPECTRA OF LANTHANIDE FLUORIDES AND OXIDES

Yu. A. Teterin, A. Yu. Teterin, A. M. Lebedev, I. O. Utkin, and A. S. Nikitin

UDC 539.194:546.654-659,661-669

Dynamic effect on the fine structure of X-ray photoelectron spectra of lanthanide oxides and fluorides is discussed. The Ln4p electron spectra are considerably complicated by the interaction between the configurations of the main one-hole and additional two-hole final states of $4p^5 4d^{10} 4f^n \leftrightarrow 4p^6 4d^8 4f^{n+1}$ *type. The effect of the nature of atoms in the nearest environment of lanthanide ions on the fine structure parameters is evaluated.*

INTRODUCTION

X-ray photoelectron studies of lanthanide compounds use not only traditional information (bond energies, intensities of fundamentals) but also fine structure characteristics, because the latter is observed in the spectra of lanthanides over the whole range of electron bond energies from 0 to 1250 eV. On the one hand, this hinders deriving traditional information from the spectra but, on the other, fine structure characteristics convey important data on the physicochemical properties of lanthanide ions and on the secondary processes accompanying electron photoemission. The dynamic effect may be one of the reasons for the fine structure of X-ray photoelectron spectra.

The dynamic effect is characterized by concurrent formation of several final states of an atom or ion during inner electron photoemission [1-9]. These additional final states arise from the giant Coster–Kronig electron transitions between the inner and outer levels during electron photoemission from the innermost level.

This effect may be illustrated by reference to a hypothetical atom A of sodium type with an electronic configuration $A1s^2 2s^2 2p^6 3s^1$ (Fig. 1). During A2*s* electron photoemission, the dynamic effect may lead to formation of a two-hole final state $E_f'(1s^2 2s^1 2p^6 3s^1)$ in addition to the main final state E_f'' $(1s^2 2s^2 2p^4 3s^2)$ of the A atom. One of the conditions of formation of this final state is multiplicity of the level energies $E_b(A2s) \cong 2E_b(A2p)$, i.e., $\Delta_1 \approx \Delta_2$ (Fig. 1). This additional final state, however, is most likely to form when the giant Coster–Kronig electron transitions occur between the levels with the same principal quantum number. In particular, for Na the probability of formation of an additional final two-hole state $1s^2 2s^2 2p^4 3s^2$ is negligibly small [10]. The dynamic effect shows itself with greater probability in M3*s* electron spectra of M3*d* element compounds [1-9]. In this case, $E_b(M3s) \cong 2E_b(M3p)$ [11]. Thus the M3*s* electron spectra can exhibit not only multiplet splitting but also the dynamic effect. This picture is observed in the Mn3*s* electron spectrum of MnO [7]. The reason for the complicated structure of the spectrum mainly lies in the formation of an additional two-hole final state $Mn3s^2 3p^4 3d^6$ [1, 9].

The dynamic effect forming an additional final state $M5s^2 5p^4 5d^{10} 6s^{n+1}$ may be assumed to underlie the complex structure of the Au5*s* and Pt5*s* electron spectra. Indeed, for electrons of these subshells, the relation $E_b(M5s) \cong 2E_b(M5p_{3/2})$ is valid to a good accuracy [11].

The spectrum structure arising from the dynamic effect is rather complex for actinide compounds [6, 12, 13] and is so diffuse in some cases that the spectrum may not be recorded.

For some lanthanide metals [14], it was shown that strong interaction between the final configurations resulting from the dynamic effect gives rise to fine structure in the Ln4*p* X-ray photoelectron spectra. A considerable contribution

---

Russian Scientific Center Kurchatov Institute. Translated from *Zhurnal Strukturnoi Khimii*, Vol. 39, No. 6, pp. 1059-1066, November-December, 1998. Original article submitted December 16, 1997.

0022-4766/98/3906-0869$20.00

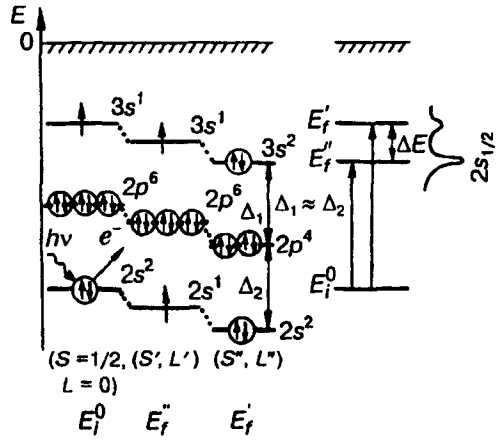

Fig. 1. Illustration of the dynamic effect leading to an interaction between the final state configurations arising from the photoemission of the A2*s* electron of the sodium-like atom A.

of inelastic electron scattering in the Ln4*p* X-ray photoelectron spectra hinders detailed analysis of the observed fine structure. Therefore, $L\gamma_{2,3}$ X-ray emission spectra of Nd and Sm in Nd_2O_3 and Sm_2O_3, respectively, were obtained in [15], and it was shown that the many-electron effects arising from the filling of the Ln4*p* hole, in particular, the giant Coster–Kronig transition $4p^5 \rightarrow 4d^8 4f^{n+1}$, bring about the fine structure of the emission spectra under analysis.

Here we investigate the fine structure of Ln4*p* and Ln3$p_{3/2}$ X-ray photoelectron spectra in lanthanide trifluorides and oxides LnF_3 and Ln_2O_3 (Ln = La–Lu, except Pm) to examine the mechanism of fine structure formation, paying special attention to the dynamic effect.

EXPERIMENTAL

X-ray photoelectron spectra were measured on an HP5950A (Hewlett–Packard) electrostatic spectrometer using monochromated Al$K_{\alpha 1,2}$ ($h\nu$ = 1486.6 eV) excitation X-ray radiation in vacuum ($1.3 \cdot 10^{-7}$ Pa) and a low-energy electron gun to compensate electrostatic charging of the samples in the course of electron photoemission from their surface at room temperature. The spectrometer resolution was measured as the fwhm of the Au4$f_{7/2}$ line (0.8 eV). The bond energies E_b (eV) are given relative to the binding energy of the C1*s* electrons of hydrocarbons on the surface of the samples, which was taken to be 285.0 eV. With an Au support, E_b(C1*s*) = 284.7 eV for E_b(Au4$f_{7/2}$) = 83.8 eV. The fwhm Γ (eV) is given relative to the C1*s* bandwidth of hydrocarbons taken to be 1.3 eV. The error in determining the binding energies of electrons and the bandwidths is up to 0.1 eV and 10% for the relative intensities.

The lanthanide oxide and trifluoride samples under study were prepared from finely dispersed samples powdered in an agate mortar and were used as thick dense layers with a mirror surface molded into titanium-supported indium. The surface of these samples may be cleaned when necessary in situ with a scrubber in vacuum (10^{-5} Pa) of the prechamber of the spectrometer.

Quantitative element analysis was performed for all samples based on the proportionality of the intensities of spectral lines to the concentration of atoms in a given sample. In this work we use the relation

$$n_i / n_j = (S_i \sigma_j / S_j \sigma_i)[(h\nu - E_{bj}) / (h\nu - E_{bi})]^{1/2}, \qquad (*)$$

where n_i / n_j is the relative concentration of the atoms under study; S_i / S_j is the relative intensity (area) of the inner electron shells of these atoms; σ_i and σ_j, E_{bi} and E_{bj} are the photoeffect and binding energy cross sections of these electrons, respectively. Experimental values were used only for the binding energies and areas; the theoretical values were employed for the photoeffect cross sections [16].

The lanthanide trifluorides LnF_3 from La to Lu, except Pm, and the oxides Ln_2O_3 were synthesized according

to the standard procedures [17]. The stoichiometric composition of all lanthanide compounds studied was determined by formula (*) and did not differ from the chemical analysis data within the limits of the error of measurement. The discussion of results uses both atomic and molecular spectral notation.

DISCUSSION OF RESULTS

Lanthanide trifluorides. In the region of Ln4*p* binding energies of the spectra of lanthanide trifluorides, lines due to Auger electrons may appear along with the C1*s* line of electrons adsorbed on the surface of hydrocarbon samples (Fig. 2, Table 1). These lines are broader and often reflect the whole series of Auger transitions. Thus the increase in the intensity starting at 350 eV in the Dy4*p* spectrum of DyF_3 may be partly due to the M_5NO electrons of the Auger transitions [18]. In the Ho4*p* spectrum, the lines of Auger electrons associated with the M_5NO transitions at $E_b > 310$ eV are so intense that the structure of the X-ray photoelectron spectrum in this region is obscured. The broad band at 400 eV in the Tm4*p* spectrum is due to the Auger electrons arising from the $M_5N_3O_3$ (395.2 eV), $M_5N_4N_5$ (391.1 eV), and $M_5N_4N_4$ (403.2 eV) transitions. The Auger electrons of the $M_5N_2O_2$ (385.8 eV) and $M_5N_1N_7$ (421.7 eV) transitions may appear in the Yb4*p* and Lu4*p* spectra, respectively.

Along with this structure, one can also observe low-intensity shake up satellites appearing on the larger-energy side of the fundamental spin doublet lines of these spectra. Also, multiplet splitting can appear in this spectral region of lanthanide trifluorides containing unpaired Ln4f^n electrons. This splitting can slightly change the bandshape of La4*p* electrons [19]. As LaF_3 and LuF_3 have no Ln4f^n electrons, the complex structure of the Ln4*p* spectra may not be explained by this splitting. For example, these spectra show a diffuse Ln4$p_{1/2}$ component. If the La4$p_{1/2}$ line is considerably diffuse, the Lu4$p_{1/2}$ spectrum will deviate from the expected spectrum to a lesser extent (Fig. 2).

A comparison between the binding energies of Ln4*p* and Ln4*d* electrons [17] shows that the relation $E_b(\text{Ln4}p) \cong 2E_b(\text{Ln4}d)$ is satisfied for the whole series of lanthanides. This and the complex structure in the La4*p* spectrum in LnF_3 may be due to the dynamic effect, i.e., may arise from the configuration interaction of $4p^5 4d^{10} 4f^n \leftrightarrow 4p^6 4d^8 4f^{n+1}$ type. Indeed, in the case of LuF_3, where the Lu4f^{14} subshell is occupied completely, the giant Coster–Kronig electron transition from the Lu4*d* subshell may occur to the next-energy empty subshell. Since the

TABLE 1. Binding Energies E_b (eV) of Ln4*p* Electrons in LnF_3 and Ln_2O_3

No.	Ln	LnF_3[a,b]				Ln_2O_3[c]		
		Ln4*p*						
1	La	198.1	203.4	213.1	(231.4)	196.3	199.4	206.4
2	Ce	208.2	223.9	243.5	250.1	207.1	214.1	
3	Pr	219.1	233.4		(251.4)	218.5		
4	Nd	229.6	246.4	259.9	(266.0)	226.4	229.7	243.5
5	Sm	251.8	269.0			250.4		
6	Eu	261.9				261.2	264.2	
7	Gd	272.7	278.7	289.4		270.6	272.6	
8	Tb	288.5	306.6		(322.6)	284.0	323.0	
9	Dy	297.3	301.3		(336.9)	292.6	294.3	335.5
10	Ho	309.9	315.0	322.6	(347.0)	308.2	314.2	
11	Er	321.3	327.3		(366.7)	320.3	326.1	362.9
12	Tm	334.4	339.6		(392.4)	333.0	337.0	
13	Yb	347.2	351.2		(399.0)	346.4	399.6	
14	Lu	361.1	414.3			359.3	412.5	

[a] Weighted means of electron energies of complex structure.
[b] The values in parentheses are the energies of satellites or shoulders.
[c] The energies of maxima are given.

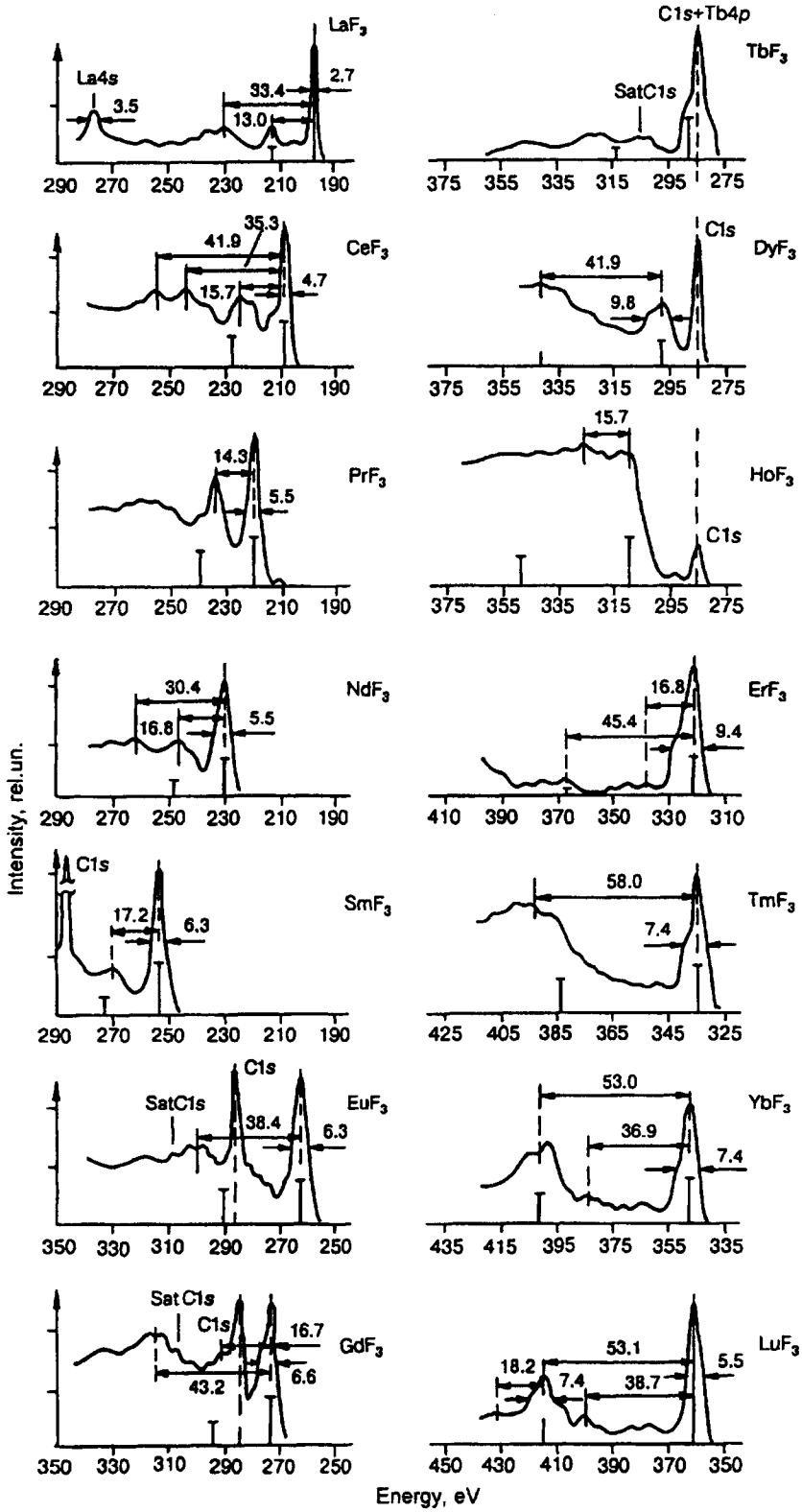

Fig. 2. Ln4*p* X-ray photoelectron spectra of lanthanide trifluorides LnF_3. The vertical bars mark the expected energies for the $Ln4p_{3/2,1/2}$ electrons neglecting the dynamic effect.

probability of this transition is smaller than that of a transition to the Ln4*f* subshell, the changes in the structure of the Lu4*p* spectrum that are due to the configuration interaction are much less significant than in the La4*p* spectrum. In the Ln4*p* spectra, the structure changes in the series La–Lu on passing from LaF_3 to LuF_3 (Fig. 2, Table 1).

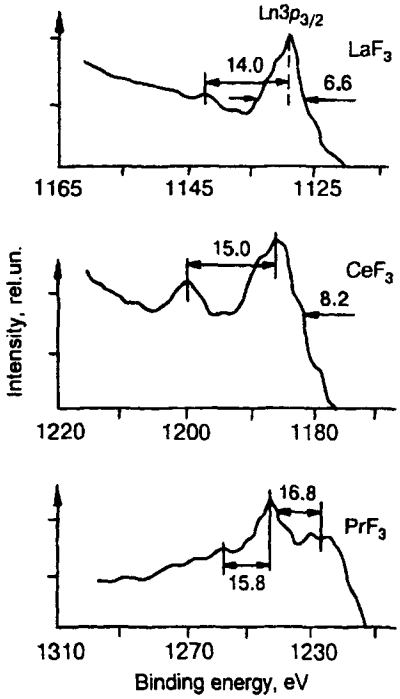

Fig. 3. $Ln3p_{3/2}$ X-ray photoelectron spectra of lanthanum, cerium, and praseodymium trifluorides.

Analogous reasoning may be applied to a treatment of the structure of the $Ln3p_{3/2}$ spectra (Fig. 3). In these spectral regions, lines of Auger electrons may appear [18]. Thus the $M_5N_1N_3$ (1125.6 eV, 1132.0 eV) lines of Auger electrons may be superimposed on the $La3p_{3/2}$ spectrum. The Auger transitions M_3NO (1184.5 eV), M_3NN (1184.5 eV), and $M_5N_1N_1$ (1202.3 eV) may appear in the $Ce3p_{3/2}$ spectrum, which can partly explain the intense maximum at 1200 eV. Auger electrons associated with M_3NN (1175.4 eV) and M_5NN_1 (1184.6 eV) type transitions may underlie the appearance of an intense broad band at 1226 eV in the $Pr3p_{3/2}$ spectrum of PrF_3.

In the spectra of $Ln3p_{3/2}$ electrons, the maxima on the high-energy side of the fundamental lines at 14-16 eV may be due to the many-electron excitation. Since $E_b(\text{Ln}3p) \cong E_b(\text{Ln}3d) + E_b(\text{Ln}4s)$ [17], in the Ln3p spectra one can expect a structure associated with a configuration interaction of $3p^53d^{10}4s^24f^n \leftrightarrow 3p^63d^94s^14f^{n+1}$ type. The experimental structure arising from the dynamic effect may be separated from the Auger lines by using an alternative source of excitation radiation. Currently, $MgK_{\alpha 1,2}$ (1253.6 eV) is the most accessible type of radiation in addition to $AlK_{\alpha 1,2}$ (1486.6 eV), but its energy is not sufficient for these spectral measurements.

Lanthanide oxides. The Ln4p spectra of the lanthanide oxides under study are analogous in structure to the spectra of lanthanide trifluorides (Figs. 2 and 4). In the Ln4p spectra of rare earth oxides, fine structure of the $Ln4p_{3/2}$ line and a significant diffusion of the $Ln4p_{1/2}$ component are observed instead of the expected doublet due to spin-orbit splitting (Table 1). For the oxides of the terminal members of the lanthanide series, in particular, Yb_2O_3, the structure of the Yb4p spectrum is nearly doublet in form, whereas the corresponding spectrum of Lu_2O_3 is mainly spin doublet (Fig. 4).

As in the case of LnF_3, this suggests that the structure of the Ln4p spectra arises from the configuration interaction of $4p^54d^{10}4f^n \leftrightarrow 4p^64d^84f^{n+1}$ type. The appearance of the additional two-hole final state $4p^64d^84f^{n+1}$ is most probable when $E_b(\text{Ln}4p) \cong 2E_b(\text{Ln}4d)$ and the Ln4f subshell is not completely occupied. This assumption is in good agreement with the experimental data for lanthanide oxides (Fig. 4). Indeed, as the electronic configurations of the La(III) and Er(III) ions are $4f^0$ and $4f^{11}$, respectively, the two-hole state $4p^64d^84f^{n+1}$ can appear from them in addition to the $4p^54d^{10}4f^n$ ground state, and a complex structure is observed in these spectra of La_2O_3 and Er_2O_3 (Fig. 4). No such additional final state is formed during the Lu4p photoemission from Lu_2O_3; this spectrum exhibits a spin doublet and satellites due to the many-electron excitation.

These results prove that the structure of the Ln4p spectra of rare-earth compounds is mainly due to the configuration interaction in the final state. However, they conflict with the assumption [20] that the structure of the

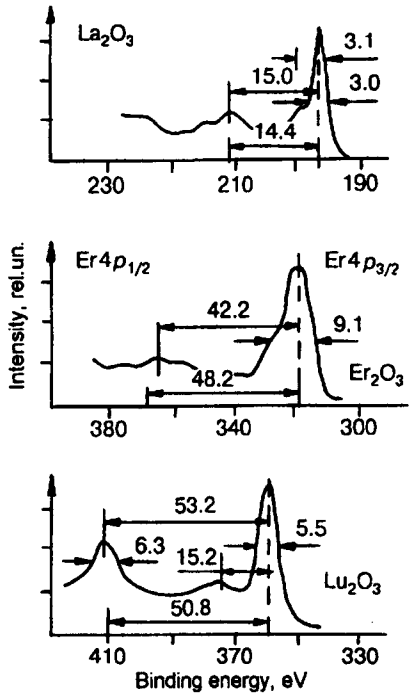

Fig. 4. Ln4*p* X-ray photoelectron spectra of Ln_2O_3. The vertical bars indicate the expected energies of $Ln4p_{3/2,1/2}$ electrons neglecting the dynamic effect.

Ln4*p* spectra of rare-earth oxides is associated with multiplet splitting. It is noteworthy that the structure of the Ln4*p* spectra of oxides differs from that of fluorides (Figs. 2 and 4, Table 1). One of the reasons for this is subexcitation into the valence band as a result of the dynamic effect. The observed structure is very complex and may not be interpreted without precision calculations, which are currently unavailable. At present we can only explain the difference by the fact that chemical binding differs between lanthanide fluorides and oxides.

As in the case of the fluorides, the Ln3*p* spectra of lanthanide oxides can exhibit the dynamic effect leading to the configuration interaction $3p^5 3d^{10} 4s^2 4f^n \leftrightarrow 3p^6 3d^9 4s^1 4f^{n+1}$ in the final state.

CONCLUSIONS

Summing up, we note that the fine structure in the Ln4*p* spectra of the lanthanide trifluorides and oxides under study arises from the dynamic effect, which is also one of the reasons for the fine structure formation in the $Ln3p_{3/2}$ spectra. In some cases, this effect as well as Auger processes causes such a strong diffusion of the Ln4*p* and Ln3*p* spectra that the structure is not discernible. The dynamic effect is of interest in physics for investigating the secondary processes accompanying electron photoemission from a substance. From chemical viewpoint, understanding the mechanisms of fine structure formation is required for correct identification of the extra lines appearing in the spectra of outer and inner electrons. Moreover, this is necessary for solving problems using other spectral methods, for example, conversion and emission spectroscopy.

Also, it should be noted that the dynamic effect is a resonance effect, i.e., $\Delta_1 \approx \Delta_2$. As is known, the effect of the nearest environment causes chemical shifts of levels and participation of the Ln4*f* electrons in chemical binding in lanthanide compounds. Therefore, the fine structure of the Ln4*p* X-ray photoelectron spectra caused by the dynamic effect will be characteristic for some particular rare-earth compounds. Since the dynamic effect involves valence electron levels, the structure of the Ln4*p* spectrum depends on the nature of atoms being the nearest neighbors of lanthanide and on the nature of chemical binding and may be used to investigate this binding.

This work was supported by RFFR.

REFERENCES

1. P. S. Bagus, A. J. Freeman, and F. Sasaki, *Phys. Rev. Lett.*, **30**, No. 18, 850-853 (1973).
2. P. S. Bagus, A. J. Freeman, and F. Sasaki, *Int. J. Quant. Chem. Symp.*, No. 7, 83-92 (1973).
3. E.-K. Viinikka and Y. Ohrn, *Phys. Rev. B*, **11**, No. 11, 4168-4175 (1975).
4. V. F. Demekhin, V. L. Sukhorukov, T. V. Shelkovich, et al., *Zh. Strukt. Khim.*, **20**, No. 1, 38-48 (1979).
5. Yu. A. Teterin, A. S. Baev, V. M. Kulakov, et al., *Abstracts of Papers from the Conference "X-Ray and X-Ray Photoelectron Spectra and Electronic Structure of Metals, Alloys, and Chemical Compounds,"* Izhevsk (1979).
6. G. Wendin, *Struct. Bond.*, **41**, 1-122 (1981).
7. Yu. A. Teterin, A. S. Baev, Yu. P. Dikov, and A. I. Gorshkov, *Dokl. Akad. Nauk SSSR*, **263**, No. 3, 610-615 (1982).
8. V. L. Sukhorukov, S. A. Yavna, V. F. Demekhin, and B. M. Lagutin, *Koordinats. Khim.*, **11**, No. 4, 510-515 (1985).
9. V. L. Sukhorukov, I. D. Petrov, V. M. Lagutin, et al., *ibid.*, **12**, No. 2, 205-206 (1986).
10. U. C. Sing, D. D. Sarma, and C. N. R. Rao, *Chem. Phys. Lett.*, **85**, 278-282 (1982).
11. K. Siegbahn, K. Nordling, A. Fahlman, et al., *ESCA, Atomic, Molecular, and Solid State, Nova Acta Regiae Societatis Scientarium Upsaliensis, Ser. IV*, Vol. 20, *Structure Studied by Means of Electron Spectroscopy*, Uppsala (1967).
12. Yu. A. Teterin, A. S. Baev, S. G. Gagarin, and V. D. Klimov, *Radiokhim.*, **27**, No. 1, 3-13 (1985).
13. Yu. A. Teterin, V. M. Kulakov, A. S. Baev, et al., *Phys. Chem. Miner.*, **7**, 151-158 (1981).
14. S. P. Kowalczyk, L. Ley, R. L. Martin, et al., *Faraday Discuss. Chem. Soc.*, **60**, 7 (1975).
15. M. Ohno and R. E. La Villa, *Phys. Rev. B*, **39**, No. 13, 8852-8857 (1989).
16. J. H. Scofield, *J. Electron. Spectrosc. Relat. Phenom.*, **8**, 129-137 (1976).
17. Yu. A. Teterin, A. S. Baev, and S. G. Gagarin, *Radiokhim.*, **28**, No. 3, 318-328 (1986).
18. F. P. Larkins, *Atom. Data Nucl. Data Tables*, **20**, No. 4, 311-387 (1977).
19. V. L. Sukhorukov, S. A. Yavna, and V. F. Demekhin, *Fiz. Tverd. Tela*, **26**, No. 7, 2172-2175 (1984).
20. B. D. Padalia, W. C. Lang, P. R. Norris, et al., *Proc. R. Soc. Lond.*, **A354**, 269-290 (1977).